# NEW WAY OF PROCESS PARAMETERS OPTIMIZATION IN SFF BASED ON DEPOSITION BY WELDING

Z. Jandric and R. Kovacevic
Research Center for Advanced Manufacturing (RCAM), Southern Methodist University
1500 International Pkwy. Suite 100, Richardson, TX 75081

## Abstract

To successfully control the welding process and to make it appropriate for solid freeform fabrication (SFF), it is necessary to fully understand the influence of the welding parameters and the geometry of the substrate on the resulting weld bead dimensions. Extensive experiments with different welding parameters and complex geometrical features such as edges and corners have been designed and completed. The experimental data show a clear correlation between the heat input, the weld bead dimensions, and the two dimensional (2D) geometrical features. This correlation may be used for on-line welding process control. It is found that the geometry of the molten pool is directly related to the heat transfer conditions determined by surrounding mass of material. A machine vision system based on a high-resolution CCD camera coaxially integrated with a gas tungsten arc welding (GTAW) torch is used to acquire the images of the molten pool. The results demonstrate the capability to adjust GTAW process parameters according to complex external and internal geometrical features of the substrate. The heat loss affected by the surrounding mass of material will be used to determine the optimal energy input.

## Introduction

In the last decade, it has been shown that solid freeform fabrication (SFF) through layered material deposition is an attractive method for 3D-object generation. Common to all layered forming techniques is the incremental nature of the material build up. The quality of each deposited layer as well as the quality of the bond between the layers determines the quality of a built part [1]. The goal of any SFF technique is the fast construction of precise parts directly from CAD drawings, or as it is often called "from computer to component" process. While most of the SFF systems still make parts from non-metallic materials, not specified by the designer of the parts, SFF based on deposition by welding overcomes this disadvantage. Several research-teams [1 – 8] have shown that this technique is capable of making diverse part shapes. Spencer et al. made a vertical wall and a hollow box. Ribeiro et al. made a 'chimney' shape, a 'bow tie' shape, and a 'pint glass' shape. Kovacevic et al. also made a thin vertical wall, cylinders, cubical 3D parts with straight channels, a 3D part with complex geometry and a 3D network of the conformal channels.

Relatively small changes to the welding parameters dramatically influence welding quality during the building of 3D parts by welding. So, an intelligent control system that controls the process parameters has to be developed. There are a number of parameters in GTAW which have a significant impact on the weld (i.e. bead) quality, such as: filler metal feeding speed, welding current, arc voltage, welding speed, shielding gas flow rate, electrode to substrate angle, type of shielding gas, shape of the tungsten electrode etc. Also, it should be noted that some of these parameters are non-linear and have transient-dependent and temperature-dependent natures. In recent years statistical design for experiments, linear regression modeling, neural network, etc. have been used to model the effects of the welding process parameters on the weld bead geometry, and it has been shown that a strong correlation between them exists [9-11].

The goals in welding based SFF are significantly different than those in metal joining. During normal welding, large depths of penetration and/or fast material deposition are desirable [12]. Some of the usual goals in the SFF based on deposition by welding are to keep the heat input as low as possible, to control the heat input in the real time, to have a small depth of penetration, to maintain uniform bead build-up, etc. Additionally, when the weld bead is deposited in the vicinity of sharp corners, heat input should be significantly lower, since the heat sink, determined by the surrounding mass of the material, is small [13]. If the heat input do not follow the conditions driven by the part geometry, unnecessary melting of already-deposited material will occur. In welding handbooks, one can find how welding parameters are related to the weld bead geometry, but all those data are intended for normal welding and can not be successfully applied to the SFF based on deposition by welding.

In this paper, extensive experiments with different welding parameters and complex geometrical features, such as edges and corners, have been designed and completed. From the experimental results, it can be observed that the heat-affected zone depends on the geometry of the substrate. In order to show the influence of the geometry on the heat transfer conditions in the vicinity of the molten pool, a new parameter called the geometrical factor is introduced. A machine vision system, based on a high-resolution CCD camera coaxially integrated into a GTAW torch, is capable of acquiring images of the molten pool in real time. A newly-developed controller uses the geometrical factor to determine the status of the mass of material around the molten pool.

## Background

The SFF based on deposition by welding (SFF – DBW) under development at Southern Methodist University is a hybrid technique – a combination of welding and cutting. The whole process of making the 3D part can be considered as relatively slow. However, if the welding parameters could be optimized, than the surface of each deposited layer would be smooth enough and many, if not all, of the layers could be deposited without introducing the milling operation, and the major disadvantage of this process could be eliminated.

To produce a flat surfaces using a dynamic process, such as GTAW, welding parameter control must be introduced. Two kind of controls can be implemented here: open-loop and closed-loop control. When closed-loop control is used, it is necessary to have an experimental database for comparing the feedback value with the optimal one. According to their difference, a controller should then react accordingly. When open-loop control is used, one should know in advance what are the most appropriate process parameters at each point (again according to a suitable database).

All of experimental data that could be found in the welding handbook [12] and in published papers are obtained by performing the experiments over a semi-infinite solid. In the semi-infinite solid (Fig.

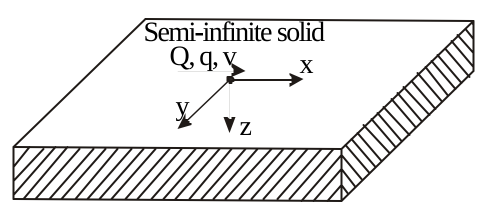


*Fig 1. Schematic presentation of semi-infinite solid*

1), the heat is propagating isotropically, since heat transfer conditions are constant during the welding. However, the building of 3D parts by welding is characterized by non-uniform heat transfer conditions (welding along edges, corners, thin substrates, etc.). It is evident that these conditions will require a new effort to form a database of optimal welding parameters as a function of the geometry of the substrate.

## Experimental Set-up

The experimental set-up of the gas tungsten arc welding process with the addition of filler metal is shown in Fig. 2. A non-consumable tungsten electrode, shielded by the inert gas (pure argon in this case) is used to strike an electric arc with a substrate. Heat generated by the electric arc is used to melt the substrate (or workpiece) and the filler metal. Filler metal is fed directly into the molten pool. Step motor (1) is used to ensure that the wire is always fed in front of the moving arc. Step motor (2) is used to control the filler metal feeding speed. A PC-based data acquisition system synchronizes the control of the step motors with a CNC machine controller, which provides precise motion of the workpiece in the X-Y plane. A machine vision system based on a high-resolution CCD camera is coaxially integrated with a GTAW torch (Fig. 3) which is capable of acquiring the images of the molten pool in real-time.

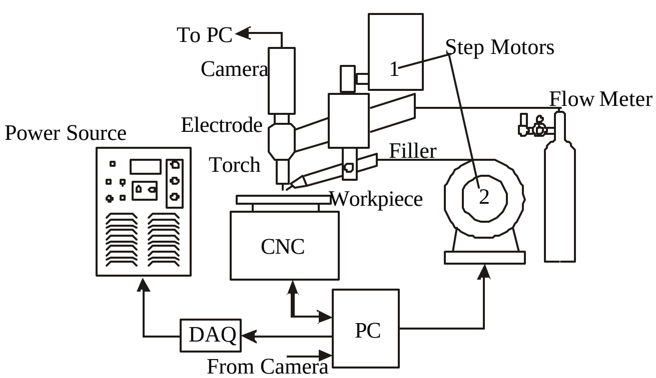


*Fig. 2 Experimental set-up for GTAW*

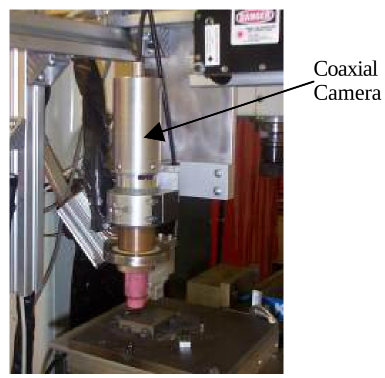


*Fig. 3 Coaxially integrated camera with torch*

## Experimental Procedure

In order to simulate different heat transfer conditions during the deposition by welding, a workpiece as a substrate is designed with different 2D geometrical features, as shown in Fig. 4. The weld beads placed along the boundary of substrate, Fig. 4b, simulate different heat sinks, from 100% for the bead placed at the flat top surface (360°) down to 12.5% for the bead placed at the 45° corner. It is evident that the welding parameters have to be controlled in order to achieve uniform weld bead geometry under different heat sink conditions.

The heat source has finite dimensions that cannot be neglected, so the distance between the edge and the electrode should be approximately half of the heat source width, which changes with the heat input [15]. In order to provide uniform heat transfer conditions during the experiment, the

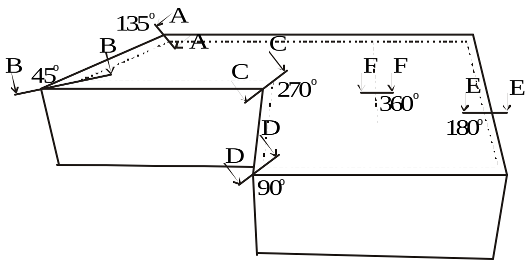


*a) Schematic presentation*

*b) after experiment*

*Fig. 4 The shape of workpiece*

workpiece is first preheated. Experience and experimental results [14] showed that the welding current and the wire feeding speed have the largest influence on the quality of the bead. Nine experiments are performed in order to analyze the affect of the welding current, the wire feeding speed, and the geometry of the substrate on the weld bead geometry. Mild steel welding wire with a diameter of 0.9 mm is used. The welding current is changed from 80 A to 160 A, with increments of 40 A. The wire feeding speed is changed from 40 cm/min to 120 cm/min, with increments of 40 cm/min.

## Experimental Results

Table 1 presents some of the experimentally obtained results. After weld beads are applied under different welding conditions, workpieces are cross-cut along the lines A-A, B-B, C-C, D-D, E-E and F-F (see Fig. 4a) in order to obtain information about the weld bead geometry. After polishing and etching the cross-sections, bead widths are measured and their relationships with respect to the welding parameters and geometrical factor are presented in Figs. 6a, 6b and 6c.

*Table 1. The bead cross-sections*

| **I[A]/ $v_f$ [cm/min]** | Angle of bead location | | | | | |
|---|---|---|---|---|---|---|
| | **45°** | **90°** | **135°** | **180°** | **270** | **360°** |
| **80/40** | 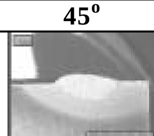 | 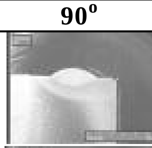 | 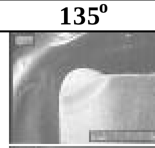 | 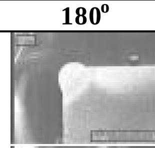 |  | 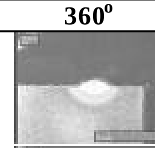 |
| **120/40** |  |  |  |  |  |  |
| **160/40** |  |  |  | 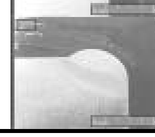 |  |  |

Experimental data are approximated with the linear functions. Each line corresponds to the bead location, such as: 45°, 90°, 135°, 180°, 270° and 360° from top-to-bottom, respectively. Increasing the welding current, while wire-feeding speed is kept constant enlarges the bead width. Also, it can be noticed that the reduction in the angle also contributes to the increase in the bead width.

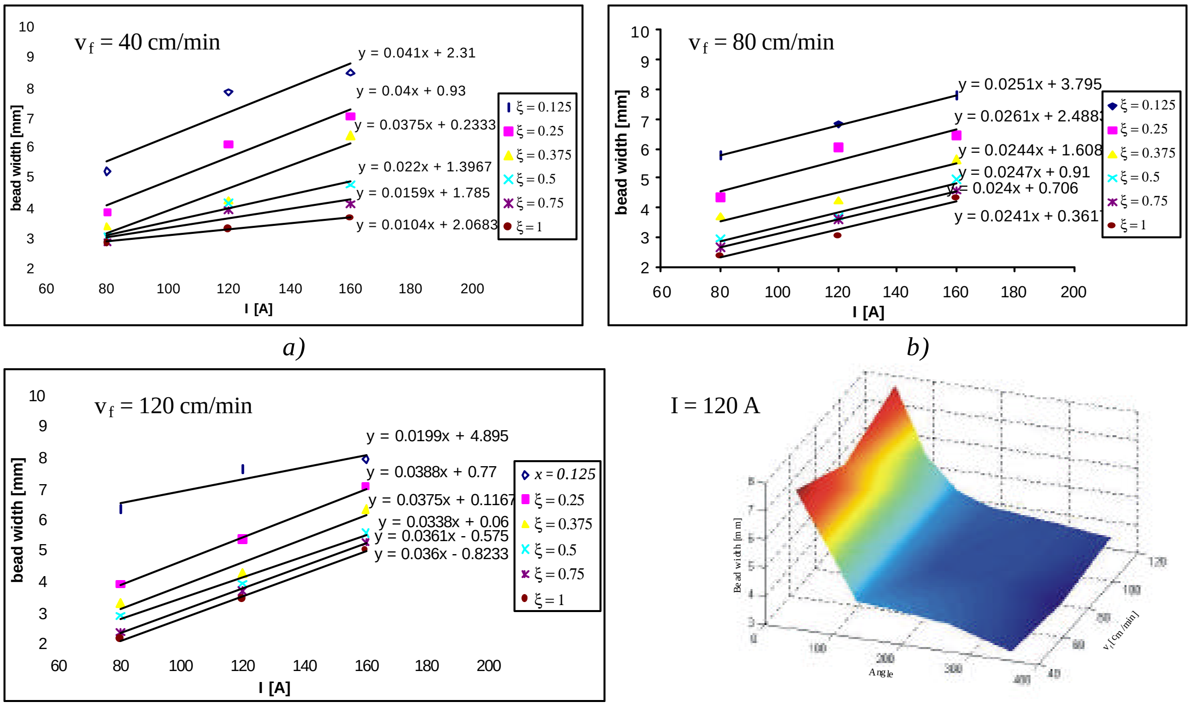


*a)* *b)* *c)* *d)*

*Fig. 5a, b, c and d – Influence of the geometry on the bead width. a, b, and c shows the bead width vs. current for three different wire feed speeds and for six different bead locations, d shows the change of the bead width when the wire feeding sped and heat sink are changed*

In order to better demonstrate the influence of the geometry of substrate on the bead width, all the experimental data obtained for an unique welding current of 120 A is presented in a three-dimensional manner (Fig. 6d). How significant this influence is can be seen if a single curve of bead width vs. angle is observed while wire feeding is kept constant. The reduction in the angle of the corner means that less surrounding material in the vicinity of the molten pool exists. By changing the angle from 360° to 45° the bead width is increased more than twice. So, an accurate model of GTAW has to take this influence into account. An outcome of this analysis is the off-line heat input planning model.

## <u>Off-line Planning and On-line Control of Heat Input</u>

Experimental results proved that local substrate geometry, i.e. vicinity of the molten pool, has the greatest impact on the bead dimensions. Since the geometry of the part to be built is known in advance, the amount of the material around an arbitrary point could be calculated. If that calculated value is provided to the controller, the heat input can be appropriately adjusted. Basically, this is the idea behind the developed off-line planning model.

In order to define the '*local geometry*', the 3D-part geometry and the net heat energy delivered to the workpiece are analyzed. Net heat energy is divided into three portions. A portion of the energy is used to melt the workpiece, the second portion is used for melting the feeding wire, and the third portion is lost to the adjacent base metal outside of the melting zone, primarily by thermal conduction. The energy lost to the base metal outside the fusion zone contributes to the formation of the heat-affected zone and to the heating of the rest of the base metal. It can be observed from the experimental results that the heat-affected zone also depends on the geometry of the substrate. Logically, when the heat input is kept constant, the greater the amount of the surrounding material, the smaller will be the heat-affected zone. The goal here is to deposit material with a constant bead height and with a uniform heat affected zone. This could be achieved by adjusting the welding parameters (mostly current) in real-time.

Heat input is the relative measure of the energy transferred per unit length of weld [14]. Typically it is calculated as the ratio of the power to the velocity of the moving heat source as follows:

$$H = \frac{60EI}{1000 \cdot S} \tag{1}$$

where, H = heat input [kJ/mm], E = arc voltage [V], I = current [A] and S = travel speed [mm/sec]. During the experiment, the arc voltage and the welding speed are kept constant, so the heat input, and therefore heat affected zone, depend only on the current. To establish the relationship between the heat input and the part geometry, the '*geometrical factor*' $\xi_G$ is introduced.

In order to define the geometrical factor, $\xi_G$, the 3D part should be represented by the 3D matrix which is generated according to the coordinates of the exterior points of the 3D solid-model. The 3D matrix consists of ones and zeros; the ones represent solid voxels and zeros represent empty voxels in the scope of the 3D solid part. The matrix is defined with the 'matrix resolution', which is the number of points per unit length. It is determined that 100 points per one inch (25.4mm) provides satisfactory results. Since all of these calculations are performed off-line, much higher resolutions can be used.

Next, the shape and the size of the heat affected zone have to be determined. It is found theoretically [15] and experimentally (Table 1) that the shape of the heat affected zone can be approximated as a half-sphere, whose radius was found experimentally to be approximately 3 mm.

The geometrical factor can be defined as:

$$x_G = \frac{V}{V_{\max}} \tag{2}$$

where, $V_{max}$ represents maximum possible number of 'ones' in the half-sphere and V is the counted number of 'ones' within the same volume. The center of the half-sphere is the point for which the welding current should be determined. So, the geometrical factor multiplied by 100 gives the percentage of the surrounding mass of the material in the vicinity of the molten pool. The accuracy of the calculated geometrical factor depends on the chosen 'matrix resolution'.

Once the geometrical factor is determined, the welding current can be selected from the experimental data-base. The results presented at Fig. 5 are particularly useful for this application. The relationship between the bead width and the welding current is approximated with the linear function. Each linear function is defined with its coefficients k and n ($y = kx + n$) and their values are given in Figs. 5a, b and c.

## Combinations of Two Controllers

A number of published results [15-19] showed that monitoring the size of the molten pool is a valuable source of information in welding. The reason why it can not be used as the sole feedback variable in SFF by welding could be demonstrated in the example shown in Fig. 6. From Fig. 6 it can be seen that welding over the channels demands three different welding-currents values in time. In the zone I, the maximal current value, $I_{max}$, should be applied in order to provide enough energy to melt the feeding wire and substrate. In the zone II, the heat input is coming close to the channel's edge. The reduction in the surrounding mass of the material necessitates a reduction in the energy needed for melting the substrate. In the zone III, the heat input is located above the channel, where the thin sheet metal is placed, and only energy for melting feeding wire is needed such that $I_{min}$ must be used. It should be noticed that decreasing the current from $I^*$ to $I_{min}$ has to be done instantaneously in order to avoid burning-through the thin sheet metal. The monitoring of the shape of the molten pool in the condition where the mass of surrounding material around the molten pool is changed abruptly will not be useful for the feedback control. However, it is shown that monitoring the molten pool under conditions of more uniform change of the surrounding mass of material around the molten pool could be successfully used as a feedback in the control of the uniformity of the bead height. The welding process is highly dynamic and depends on the many transient and temperature dependent parameters that are difficult to predict. These parameters are considerably less influential than the part geometry, but they still affect the quality of the bead. So, the need for an additional 'independent' controller that will provide more uniform quality of deposition by welding is necessary. Fig. 7 shows the images of the molten pool obtained for the constant welding current and constant wire feeding speed, but still, the size as well as the shape of the molten pool fluctuates significantly.

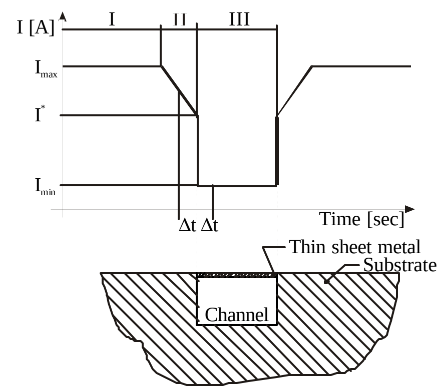


*Fig. 6 Current vs. time is related to the part geometry*

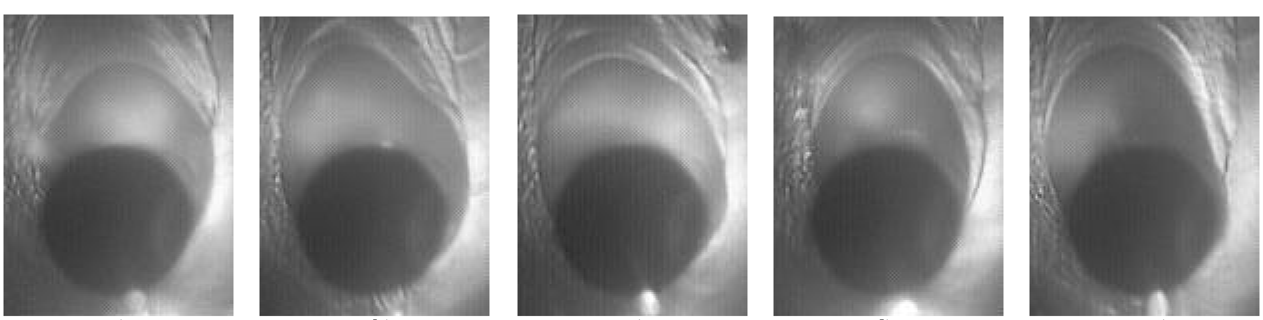

*a) b) c) d) e)*

*Fig. 7 Images of the fluctuating molten pool obtained for the same welding parameters*

Architecture of the developed controller to control welding current for SFF - DBW is showed in Fig. 8. Before the controller updates the welding current, data about the heat transfer conditions in the vicinity of the molten pool has to be provided, and this information is inherent in the value of the geometrical factor. Each time the calculated geometrical factor is referenced (Fig. 8). From the definition of the geometrical factor it follows that, if the geometrical factor is less than one, the selection of the corresponding welding current has to be made off-line. If it is one, monitoring of the size of the molten pool by machine vision is used to control the uniformity of the bead height. Overall performance of the designed control strategy is shown in Fig. 9, where welding current vs. time, and voltage vs. time diagrams are presented.

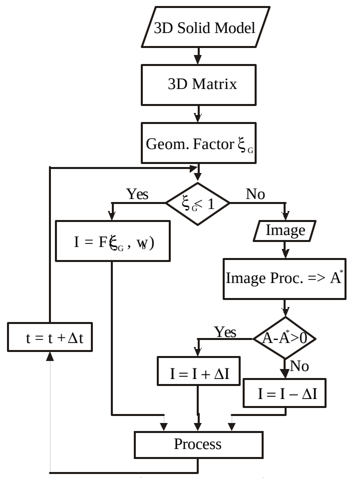


*Fig. 8 Information flow in the designed controller*

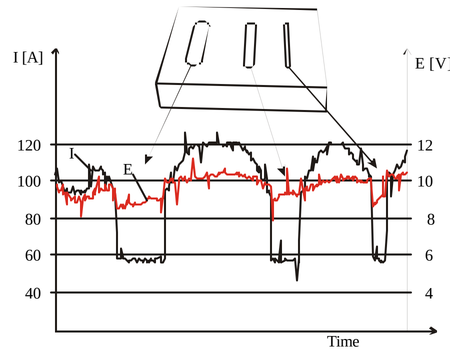


*Fig. 9 Current and voltage vs. time*

The verification of the designed controller is performed on the samples shown in Fig. 10. Three grooves with different widths (6.5 mm, 3.8 mm, and 1.7 mm) are milled in the block of mild steel with sizes of 63.8 mm × 50.6 mm × 12.7 mm. The depth of the grooves is 7.8 mm. The grooves are filled up with casting sand and covered with 1mm thick steel sheet metal. The goal is to make a build up of material over the top surface of this sample by depositing material in the form of layers by SFF – DBW. In the case of welding without a controller or any pre-selected welding parameters will generate excessive heat and the thin sheet metal covers will burn through, as it is shown in the Fig. 10b. Fig. 10c shows the results of the build up in the case when the selection of the welding current is done in advance based on the geometry, along the torch path. The burn-through is avoided but the uniformity of the build-up layer is not achieved. Fig. 10d shows the results of the control strategy shown in Fig. 8. In the case when the geometrical factor along the torch path is less than one, the welding current is selected in advance. However,

*a)* *b)* *c)* *d)*

*Fig. 10 Weld deposition over the channels*

if this factor is equal to one, then the welding current will be selected on-line based on the area of the molten pool obtained in real-time by incorporated machine vision. The outcome of this control strategy is a very uniform height of built layer over the channels. The same strategy will be applied to the building of a layer with specified external and internal boundaries of material which are deposited by welding. The results of building a part consisting of very sharp corners are shown in Fig. 11.

## Building a Test Part

The controller is challenged with depositing filler metal over a complex geometry (Fig. 11). A 3D part with sharp corners is successfully built. Building this part can be divided into several stages: a) making 3D solid model, Fig. 11a, b) slicing it, Fig. 11b, c) automatically generating G-code for the planned torch path Fig. 11c, d) depositing material along the external boundary of the layer where the welding current is selected in advance based on the value of the geometrical factor along the torch path, Fig. 11d, e) depositing material inside of the border contour, therby activating the machine vision system that will feed the data into the controller for selecting the welding current in real time, Fig. 11e, f) final shape of the part after end and face milling is done, Fig. 10f.

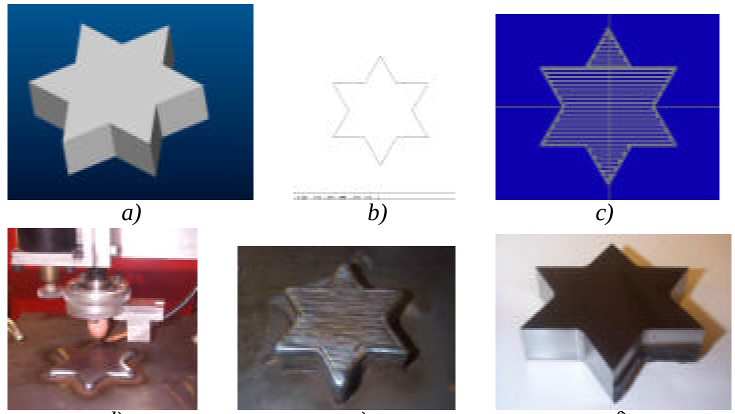


*Fig. 11. Building a Test Part*

## Conclusion

Extensive experiments with different welding parameters and complex geometrical features such as edges, corners, and channels have been designed and completed, and an experimental database has been created. A new parameter, named the geometrical factor, is introduced, that reflects on the local geometry of the substrate. A machine vision system based on a high-resolution CCD camera which is integrated into the GTAW torch is used for monitoring the size of the molten pool. The heat input controller is developed and tested. The controller is characterized by two branches. The off-line control branch is activated when the torch is following the external and the internal boundaries of the layer. In that case, the welding current is specified in advance based on the known shape layer boundary. The other branch of the controller, the on-line branch, is activated during the filling of the surface surrounded by the external and the internal boundaries. In this case, the shape of molten pool captured by the machine vision system is used as feedback for selecting the corresponding welding current.


## Acknowledgment

This work was financially supported by THECB, Grant $N_o$. 003613-0022001999, NSF, Grants $N_o$. DMI – 9732848 and DMI – 9809198, and the U.S. Department of Education, Grant $N_o$. P200A-80806-98.

# References


(1) Spencer, J.D., Dickens, P.M., and Wykes, C.M., (1998). Rapid prototyping of metal parts by three-dimensional welding, *ImechE Proc. Part B, Journal of Engineering Manufacture*, Vol. 212, pp. 175-182.

(2) Dickens, P., Cobb, R., Gibbson, I., and Pridham, M., (1993). Rapid Prototyping Using 3D Welding, *Journal of Design and Manufacturing*, Vol. 3, No. 1, March, pp. 39-44.

(3) Merz, R., Prinz, F., Ramaswami, K., Terk, M., and Weiss, L., (1994). Shape Deposition Manufacturing, *Proceedings of the Solid Freeform Fabrication Symposium*, University of Texas, Austin, Texas, August 8-10.

(4) Karunakaran, K., Shanmuganathan, P., Roth-Koch, S., and Koch, K., Direct Rapid Prototyping Tools, *Proc. of the SFF Symposium*, University of Texas, Austin, TX, August 1998, pp. 105-112.

(5) Ribeiro, A. F. M., Norrish, J., (1996). Rapid Prototyping Process using Metal Directly, *Proceedings of Solid Freeform Fabrication, Symposium*, 12-14 August, Austin, pp. 249-256, ISSN 1053-2153.

(6) Kovacevic, R., (2001). Rapid Manufacturing of Functional Parts Based on Deposition by Welding and 3D Layer Cladding, *Proc. of the MoldMaking Conference*, April 3-5, Rosemont, IL, presented by the MoldMaking Technology Magazine, pp. 263-276.

(7) Kmecko, I., Hu, D., and Kovacevic, R., (1999). Controlling Heat Input, Spatter and Weld Penetration in GMA Welding for Solid Freeform Fabrication, *Proceedings of the 10th Solid Freeform Fabrication, Symposium*, August, Austin.

(8) Kmecko, I.S., Kovacevic, R., and Jandric, Z., (2000). Machine Vision Based Control of Gas Tungsten Arc Welding for Rapid Prototyping, *Proceeding of the 11th Solid Freeform Fabrication, Symposium*, August, pp. 578-584.

(9) Starling, M.D., Marques, V., and Modenesi, J., (1995). Statistical modeling of narrow gap gas tungsten arc welding with magnetic arc oscilation, *Journal of Material Processing*, 51, pp. 37-49.

(10) Zeng, X.M., Lucas, J., and Fang, M.T.C., (1993). Use of neural networks for parameter prediction and quality inspection in tungsten inert gas welding, *Transaction of the Institute of Measurement and Control*, 15(2), pp. 87-95.

(11) Million, K., Datta, R., Zimmermann, H., (1986). Method of manufacture of a design piece by form creating deposition welding and a design piece manufactured by this method, *European Patent Office*, Publication number: 0 172 309 A1.

(12) Welding Handbook – Part 1, eighth edition, volume 2, American Welding Society, Miami, 1996.

(13) Radaj, D., (1992). Heat Effects of Welding – Temperature Field, Residual Stress, Distortion, *Springer-Verlag Berlin Heidelberg*, printed in the USA.

(14) Scot, R., (1999) A Look at Heat Input, *Welding Innovation*, Vol. XVI, No. 1, pp. 8-11.

(15) Kovacevic, R., Zhang, Y.M., (1995) Real-Time Image Processing for Monitoring of Free Weld Pool Surface, *Journal of Manufacturing Science and Engineering*, Vol. 119, pp. 161-169.

(16) Kovacevic, R., Zhang, Y.M., Ruan, S., (1995). Sensing and Control of Weld Pool Geometry for Automated GTA Welding, *Transaction of the ASME*, Vol. 117, pp. 210-222.

(17) Richardson, R.W., Gutow, D.A., Anderson, R.A. and Farson, D.F., (1984). Coaxial Arc Weld Pool Viewing for Process Monitoring and Control, *Welding Journal*, March 1984, pp. 43-51.

(18) Brzakovic, D., Khani, D.T., Awad, B., (1992). A Vision System for Monitoring Weld Pool, *Proceedings of the 1992 IEEE, International Conference on Robotics and Automation*, Nice, France, May, 1992, pp. 1609-1614.

(19) Chen, S.B., Lou, Y.J., Wu, L., Zhao, D.B., (2000). Intelligent Methodology for Sensing, Modeling and Control of Pulsed GTAW: Part I – Bead-on-Plate Welding. *Welding Research Supplement*, June 2000, pp. 151-s, 163-s.